Article

Cell Reports

Neurobeachin and the Kinesin KIF21B Are Critical for Endocytic Recycling of NMDA Receptors and Regulate Social Behavior

Graphical Abstract

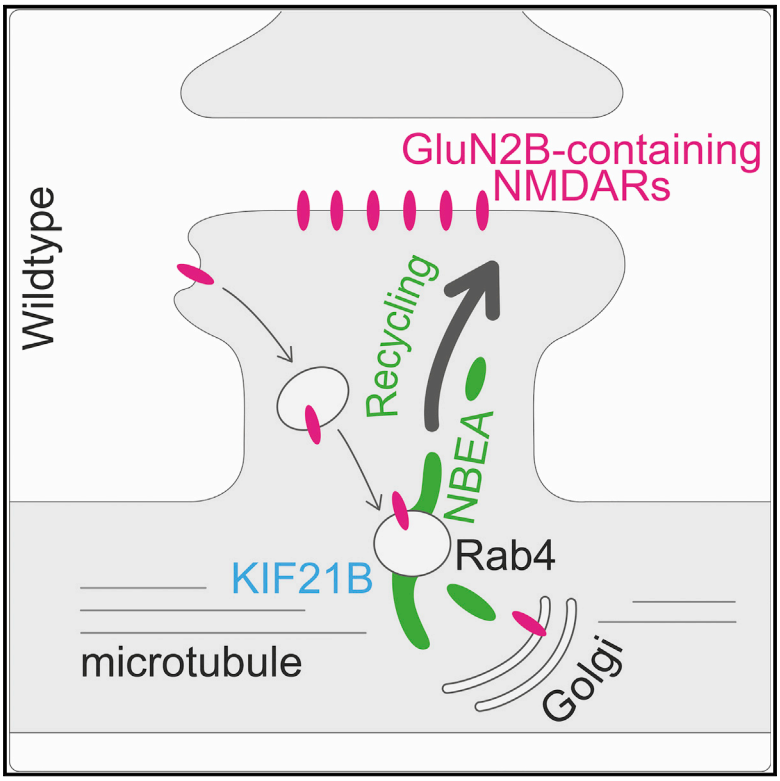

Authors

Kira V. Gromova, Mary Muhia, Nicola Rothammer, ..., Olga Shevchuk, Thomas G. Oertner, Matthias Kneussel

Correspondence

matthias.kneussel@zmnh.uni-hamburg.de

In Brief

Gromova et al. functionally link the autism risk factor neurobeachin with KIF21B and endosomal pathways. Dynamic NBEA localizes at recycling endosomes and enters synapses in an activity-dependent manner. NBEA and KIF21B regulate NMDAR cell surface expression, and similar to NBEA mutants, KIF21B depletion induces social abnormalities linked to autism.

Highlights

- NBEA associates with endosomal recycling factors and labels tubules at endosomes
- NBEA transiently enters synapses and is regulated by KIF21B and dynein motors
- NBEA and KIF21B regulate GluN2B-containing NMDA receptor cell surface expression
- Similar to NBEA, KIF21B is relevant for ASD-related social behavior

Gromova et al., 2018, Cell Reports *23*, 2705–2717
May 29, 2018
https://doi.org/10.1016/j.celrep.2018.04.112

CellPress

Cell Reports
Article

Neurobeachin and the Kinesin KIF21B Are Critical for Endocytic Recycling of NMDA Receptors and Regulate Social Behavior

Kira V. Gromova,[1] Mary Muhia,[1] Nicola Rothammer,[1] Christine E. Gee,[2] Edda Thies,[1] Irina Schaefer,[1] Sabrina Kress,[1] Manfred W. Kilimann,[3] Olga Shevchuk,[4,5] Thomas G. Oertner,[2] and Matthias Kneussel[1,6,*]
[1]Department of Molecular Neurogenetics, Center for Molecular Neurobiology, ZMNH, University Medical Center Hamburg-Eppendorf, Hamburg, Germany
[2]Department of Synaptic Physiology, Center for Molecular Neurobiology, ZMNH, University Medical Center Hamburg-Eppendorf, Hamburg, Germany
[3]Department of Molecular Neurobiology, Max-Planck Institute for Experimental Medicine, Göttingen, Germany
[4]Cellular Proteomics Research Group, Helmholtz Centre for Infection Research (HZI), Braunschweig, Germany
[5]Leibniz Institute for Analytical Sciences, ISAS, Dortmund, Germany
[6]Lead Contact
*Correspondence: matthias.kneussel@zmnh.uni-hamburg.de
https://doi.org/10.1016/j.celrep.2018.04.112

SUMMARY

Autism spectrum disorders (ASDs) are associated with mutations affecting synaptic components, including GluN2B-NMDA receptors (NMDARs) and neurobeachin (NBEA). NBEA participates in biosynthetic pathways to regulate synapse receptor targeting, synaptic function, cognition, and social behavior. However, the role of NBEA-mediated transport in specific trafficking routes is unclear. Here, we highlight an additional function for NBEA in the local delivery and surface re-insertion of synaptic receptors in mouse neurons. NBEA dynamically interacts with Rab4-positive recycling endosomes, transiently enters spines in an activity-dependent manner, and regulates GluN2B-NMDAR recycling. Furthermore, we show that the microtubule growth inhibitor kinesin KIF21B constrains NBEA dynamics and is present in the NBEA-recycling endosome-NMDAR complex. Notably, *Kif21b* knockout decreases NMDAR surface expression and alters social behavior in mice, consistent with reported social deficits in *Nbea* mutants. The influence of NBEA-KIF21B interactions on GluN2B-NMDAR local recycling may be relevant to mechanisms underlying ASD etiology.

INTRODUCTION

Endosomal recycling of receptors is essential to synaptic function and plasticity (Collingridge et al., 2004). Upon internalization, receptors may be targeted for lysosomal degradation or revert to the plasma membrane from recycling endosomes (Sheff et al., 1999). The relevance for endocytic recycling mainly stems from AMPA receptor (AMPAR) studies (Correia et al., 2008; Huganir and Nicoll, 2013; Park et al., 2004; van der Sluijs and Hoogenraad, 2011), which highlight recycling endosomes as intracellular submembrane reserve pools that modulate long-term potentiation (LTP) (Granger et al., 2013; Kneussel and Hausrat, 2016; Park et al., 2004; Petrini et al., 2009). Little is known about endocytic trafficking of NMDA receptors (NMDARs) at synapses (Cheng et al., 2013; Gu and Huganir, 2016; Piguel et al., 2014; Suh et al., 2010), although recent studies show that Rab activity potentiates NMDAR function (Cheng et al., 2013) and that dominant-negative Rab mutants block distinct steps of NMDAR endocytosis and recycling (Gu and Huganir, 2016). Besides classical recycling, the retromer complex mediates the recycling of receptors via the trans-Golgi network (TGN) (Mikhaylova et al., 2016).

The microtubule (MT)-based motors kinesin and cytoplasmic dynein form complexes with other proteins to transport cargo along the microtubule cytoskeleton (Hirokawa et al., 2010; Kneussel et al., 2014). For example, the biosynthetic-to-synapse transport of NMDARs is mediated by the KIF17 motor (Guillaud et al., 2008). Kinesin and dynein are prominent Rab effector proteins, indicating that Rab GTPases connect to motors either directly or indirectly via adaptor molecules (Horgan and McCaffrey, 2011). Certain kinesins are also involved in microtubule depolymerization (Hirokawa et al., 2010). For instance, KIF21B acts both as processive motor and microtubule growth-pausing factor (Muhia et al., 2016; van Riel et al., 2017). KIF21B is shown to regulate synapse morphology and function, yet how KIF21B interacts with other protein components to ensure normal synaptic function remains unclear.

Neurobeachin (NBEA) is a brain-enriched 327 kDa multidomain protein. Its gene has been linked to autism spectrum disorders (ASDs) (Castermans et al., 2003), which are characterized by behavioral inflexibility, altered cognition, and social interaction abnormalities (Poon and Sidhu, 2017). While *Nbea* loss of function in *Drosophila* mutants alters social behavior (Wise et al., 2015), *Nbea* haploinsufficiency is sufficient to induce cognitive dysfunction and ASD-like phenotypes in mice (Nuytens et al., 2013). These abnormalities are attributed to deficient NBEA function on the genesis and maintenance of synapses. Loss of NBEA causes aberrant clustering of synaptic proteins

on dendritic shafts and decreased actin enrichment in spines (Niesmann et al., 2011). Consequently, NBEA deficiency induces significant spine loss and corresponding deficits in synaptic efficacy and plasticity (Farzana et al., 2016; Medrihan et al., 2009; Nair et al., 2013; Niesmann et al., 2011; Nuytens et al., 2013).

NBEA is proposed to influence synaptic function and plasticity by regulating the targeting of receptors to synapses from biosynthetic compartments. It is readily identified at endoplasmic reticulum (ER)-Golgi compartments (Nair et al., 2013; Wang et al., 2000) and is predicted to function as a scaffold and/or anchor in regulating secretory-biosynthetic pathways (Wang et al., 2000). Also, NBEA is suggested to regulate post-Golgi glycine receptor (GlyR) trafficking in affiliation with VPS35 (del Pino et al., 2011). Although evidence for physical associations is pending, NBEA is responsible for trafficking of other receptor types as evidenced by decreased surface expression of $GABA_A$, AMPA, and NMDARs in NBEA deficient neurons (Farzana et al., 2016; Nair et al., 2013). Indeed, these receptors accumulate in distinct biosynthetic compartments (Nair et al., 2013), consistent with the proposal that NBEA may target different receptor types via distinct pathways (Farzana et al., 2016). These discrete functions may depend on interactions with specific partners (del Pino et al., 2011; Lauks et al., 2012) that modulate cargo specificity and trafficking.

Presently, it is unclear whether NBEA function is restricted to biosynthetic-to-plasma membrane trafficking or may include additional local roles in surface re-insertion and recycling of receptors. NBEA was previously detected at synaptic contacts (Wang et al., 2000). Furthermore, NBEA dendritic localization and its dispersal in dendrites upon neuronal stimulation (Nair et al., 2013) are strongly suggestive of a role for NBEA in this respect. Thus far, potential interacting partners and corresponding events are unclear. Studies in *C. elegans* implicating NBEA in endosomal trafficking in epithelial cells (de Souza et al., 2007) suggest that such a role may be applicable to submembrane trafficking of internalized receptors at synapses. Whether this is dependent on NBEA dynamics and mobility is currently unexplored.

Here, we demonstrate a role for NBEA in endosome dynamics and endocytic recycling of GluN2B-containing NMDARs. We show that NBEA interacts with GluN2B-NMDARs in a complex with post-Golgi recycling factors Rab4 GTPase and retromer component VPS35. NBEA is a highly dynamic component of membrane tubules that extend from Rab4 recycling endosomes and enters dendritic spines in an activity-dependent manner. NBEA also colocalizes with GluN2B at synaptic sites and governs its cell surface recycling. Interestingly, we found that the kinesin KIF21B interacts with NBEA in the GluN2B-Rab4-VPS35 complex and critically regulates the dynamics of NBEA motility. We demonstrate the relevance of NBEA-KIF21B further by showing that both proteins are required for cell surface expression of NMDARs. Furthermore, KIF21B knockout decreases social approach and recognition, consistent with notable deficits in *Nbea* mutants (Nuytens et al., 2013). Altogether, our study suggests that NBEA and KIF21B are recruited to the endosomal trafficking machinery to regulate NMDAR surface expression, which may be of relevance to mechanisms underlying ASD etiology.

RESULTS

NBEA Is Located at Newly Forming Tube-Shaped Vesicles and Enters Active Synapses in Response to Glutamate

To determine the subcellular distribution of endogenous NBEA in neurons, we analyzed the colocalization of NBEA with the dendrite marker MAP2. NBEA displayed punctate distribution in dendrites (Figure 1A) and was enriched at the somatic Golgi compartment identified through COPI-coated vesicles (Figure 1B). Brain fractionation revealed prominent NBEA levels in vesicle-enriched P3 pellets and P2 plasma membrane fractions (Figure 1C). Likewise, NBEA signals were detected at spine synapses (Figure 1D).

We extended our assessment of NBEA expression by using live imaging in neurons transfected with N-terminal GFP- or mCherry-NBEA fusion proteins (Figure S1A). Both fusion proteins mimicked the subcellular distribution of endogenous NBEA in dendrites and at perinuclear areas (Figures 1E and S1B–S1D). Observed puncta were mobile in both neurons and COS-7 fibroblasts (Figures 1F and S1E; Videos S1 and S2). Confocal and total internal reflection fluorescence (TIRF) imaging confirmed extensive distribution of GFP-NBEA in cells (Figure 1G, left) with some located close to the cell surface (Figure 1G, right).

Because GFP-NBEA particles displayed motility in the range of 0.25–1.0 μm/s (Video S1; Figures 2A and 2C), we examined whether this was dependent on either intact microtubules or actin filaments. The disruption of microtubules with nocodazole significantly decreased NBEA particle velocity by 36% (Figures 2B and 2C), indicating that intact microtubules are essential for NBEA motility. Notably, in fibroblasts (Figure 2D, left; Video S2) and neurons (Figure S2A; Video S1), GFP-NBEA was located at both newly forming and pre-existing tubular vesicles that were mobile and traveled throughout the cell. Nocodazole markedly inhibited the formation and displacement of these tubular vesicles and altered the characteristic tubule-like extensions, leading to more rounded vesicles (Figure 2D, middle, and Figures 2E and 2F). Although the inhibition of actin polymerization with cytochalasin D did not affect tubule formation, it induced a significant increase in tubule length (Figure 2D, right, and Figure 2E). These observations indicate that the outgrowth and motility of NBEA-containing tubules is mainly microtubule dependent and may involve additional proteins of the microtubule transport machinery.

Because various proteins, organelles, and microtubules enter dendritic spines in an activity- and NMDAR-dependent manner (Esteves da Silva et al., 2015; Hu et al., 2008), we examined whether mobile NBEA puncta enter dendritic spines and whether synaptic activity might influence NBEA particle mobility. Live imaging (5 min) under basal conditions revealed GFP-NBEA particle entry in 7.5% of observed spine heads (Figure 2G; mCherry: volume marker). Particle entry into spine protrusions was transient and lasted several seconds (Figure 2H). To verify that NBEA-positive spines indeed represent functional synapses, we performed a synaptotagmin antibody-uptake assay (Figure 2I). Interestingly, GFP-NBEA particles entered both active (40%) and inactive (60%) synapses (Figure 2I; Video S3). Upon stimulation with glutamate (1 μM, 5 min), NBEA particle entry into spines doubled

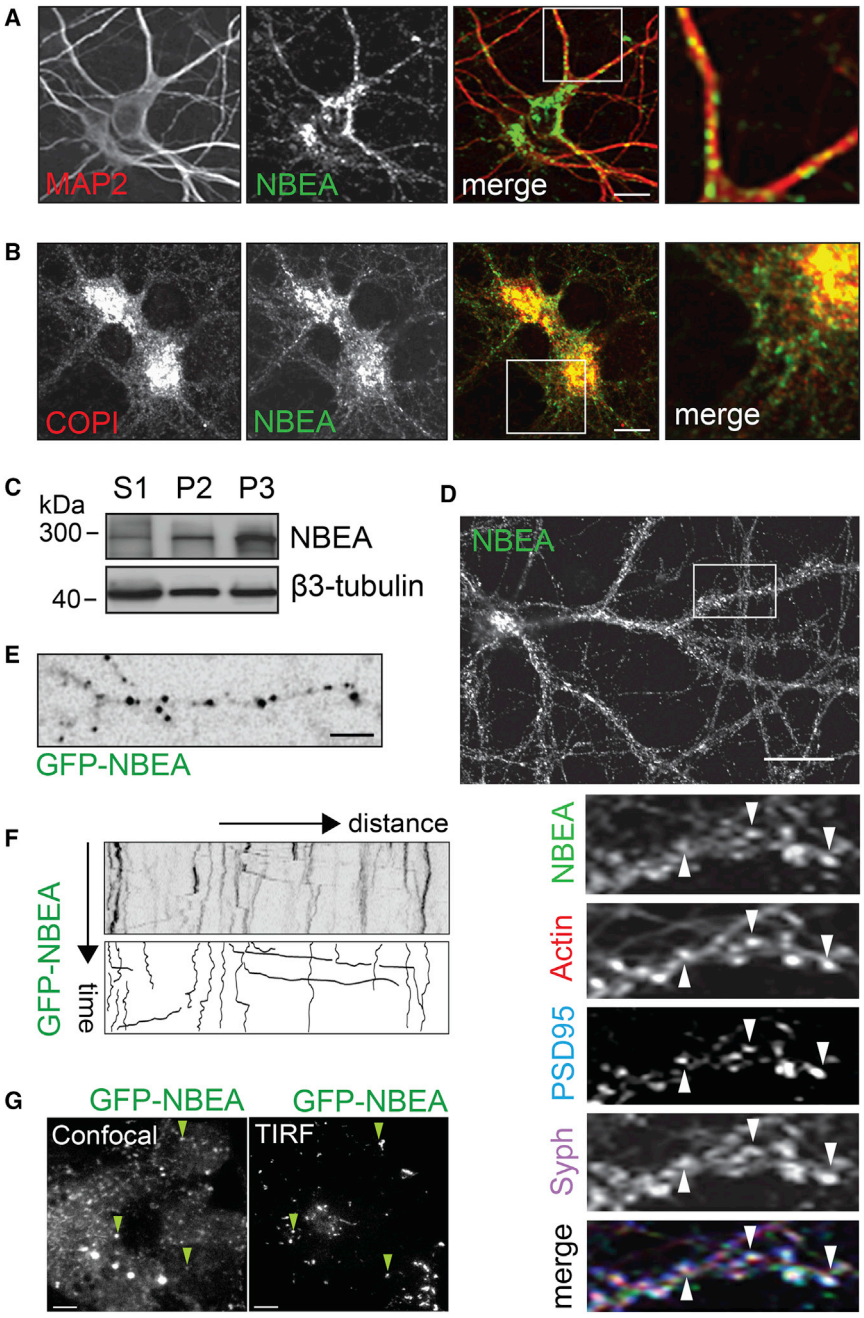

Figure 1. Neurobeachin Is Located at Neuronal Dendrites and Synaptic Sites

(A) Neurons co-labeled with NBEA (green) and the dendritic marker MAP2 (red).

(B) Neurons co-labeled with NBEA (green) and the Golgi vesicle marker COP1 (red).

(C) Analysis of NBEA content in subcellular fractions of adult mouse brain. S1, supernatant (1,000 × g); P2, plasma membrane-enriched pellet (10,000 × g); P3, vesicle-enriched pellet (100,000 × g); loading control, β3-tubulin.

(D) Neurons co-stained with NBEA (green), actin (red), PSD95 (blue), and synaptophysin (purple); 28.6 ± 1.39% of NBEA is detected at spine synapses (arrowheads) (n = 22 cells, n = 3 experiments).

(E) GFP-NBEA in neuronal dendrites at day *in vitro* (DIV) 13.

(F) Kymograph showing GFP-NBEA anterograde and retrograde particle mobility in neurites.

(G) GFP-NBEA expression in COS7 cells as observed with confocal (left) or TIRF (right) microscopy. Arrowheads denote NBEA close to the plasma membrane.

Scale bars: 2 μm (E), 5 μm (G), and 10 μm (A, B, and D). See also Figure S1.

(13%; Figures 2J and 2K), without altering particle velocity (Figure S2B). Thus, synaptic activity promotes NBEA spine entry, suggesting possible cargo delivery into synapses.

The Microtubule Motor Proteins KIF21B and Dynein Differentially Regulate NBEA Motility

Because microtubule-based transport often involves a complex of several proteins (Hirokawa et al., 2010), it is likely that NBEA trafficking includes additional factors of the microtubule transport machinery. Also, because NBEA motility is microtubule dependent (Figure 2), we speculated that microtubule-regulatory proteins might influence NBEA motility. We therefore performed NBEA co-immunoprecipitation (coIP), followed by mass spectrometry (MS) analysis to probe for putative proteins that may associate with NBEA. We identified potential candidates, many of which represent key factors of the subcellular and endocytic trafficking machinery, cytoskeletal transport, trafficking adapters, and GTPases (Table S1). We focused our investigation on the kinesin-4 family member KIF21B, which emerged as a candidate in MS analysis (Table S1) and has been shown to regulate microtubule dynamics (Ghiretti et al., 2016; Muhia et al., 2016; van Riel et al., 2017). IP with a NBEA-specific antibody led to coIP of endogenous KIF21B from brain lysate (Figure 3A). Reciprocal IP with a KIF21B-specific antibody co-immunoprecipitated endogenous NBEA (Figure 3A), thus confirming the MS results. In neurons, colocalization analysis using KIF21B and NBEA fusion proteins yielded substantially overlapping peaks along dendrites (Figures 3B and 3C). We therefore examined the relevance of KIF21B on GFP-NBEA particle mobility in neurons derived from *Kif21b* wild-type (+/+) and *Kif21b*-knockout (−/−) mice. Although NBEA was equally expressed in both genotypes (Figures S3A and S3B), GFP-NBEA particles traveled with significantly higher velocity (Figures 3D and 3E) and over longer distances (Figures 3D and 3F) in *Kif21b*-knockout relative to wild-type neurons. Anterograde versus retrograde transport was comparable for

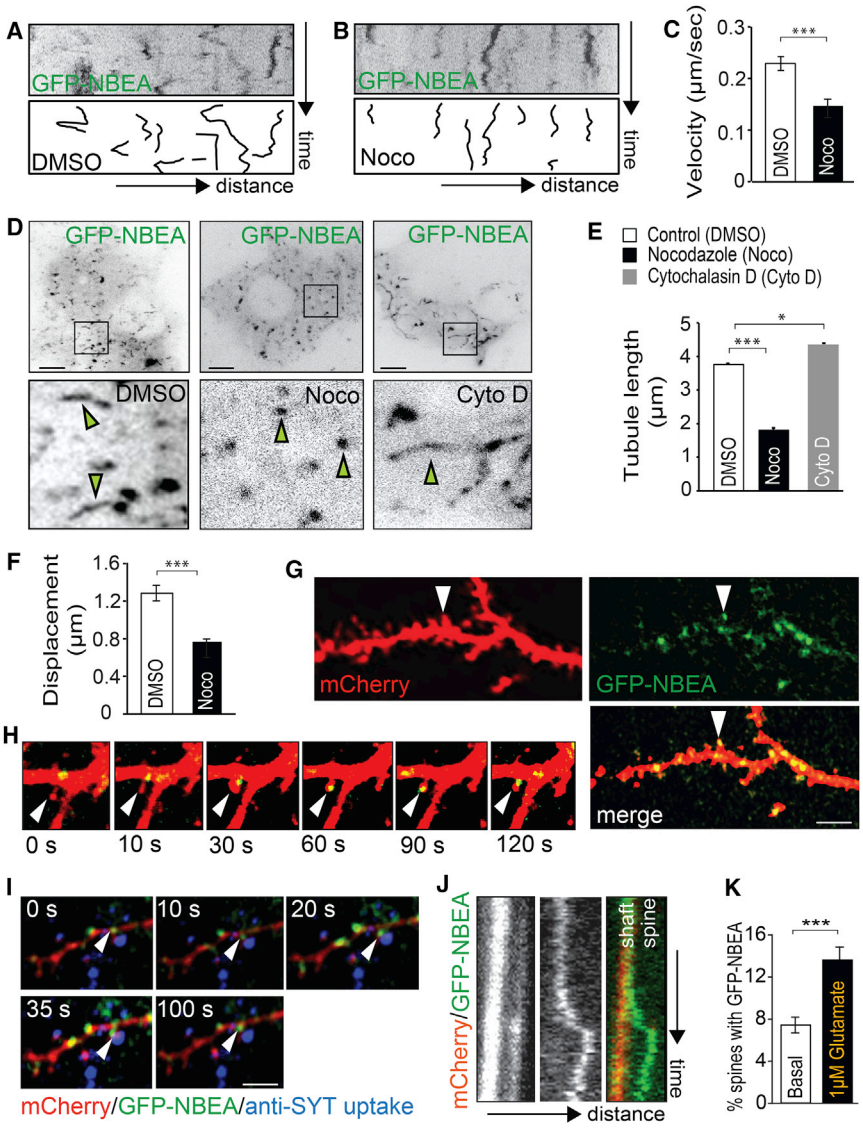

Figure 2. Neurobeachin Labels Nocodazole-Sensitive Tubules and Enters Active Spines in an Activity-Dependent Manner

(A and B) Kymographs of GFP-NBEA particle mobility in COS7 cells treated with DMSO (A) or nocodazole (Noco) (B).

(C) Quantification of GFP-NBEA velocity (n = 18 [DMSO] and n = 28 [Noco] cells, n = 3 experiments each).

(D) GFP-NBEA expressing COS7 cells treated with DMSO, Noco, or cytochalasin D (CytoD). Boxed regions: shown below.

(E) Quantification of GFP-NBEA tubule length (n = 18 [DMSO] and n = 28 [Noco] cells, n = 26 [CytoD] cells, n = 3 experiments each).

(F) Quantification of GFP-NBEA displacement (n = 18 [DMSO] and n = 28 [Noco] cells, n = 3 experiments each).

(G) Dendrite of a neuron expressing mCherry (red, volume marker) and GFP-NBEA. Arrowheads denote GFP-NBEA in dendritic spines.

(H) Neurons expressing mCherry (red) and GFP-NBEA (green). Arrowheads depict GFP-NBEA signal that enters and leaves a dendritic spine within seconds.

(I) Neuron expressing mCherry and GFP-NBEA. Active presynaptic terminals internalize Cy5-labeled synaptotagmin-1 antibodies (anti-SYT) while recycling their neurotransmitter (activity-dependent uptake assay). Arrowheads denote GFP-NBEA signal that attaches and detaches from a blue signal representing an active terminal bouton (n = 23 cells, n = 5 experiments).

(J) Kymograph of GFP-NBEA particle mobility in neurons expressing mCherry. The green signal leaves the shaft and enters the spine over time.

(K) Quantification of GFP-NBEA spine entries under basal and activity-dependent conditions (n = 29 cells [basal], n = 33 cells [glutamate], n = 4 experiments each).

All quantified values represent mean ± SEM. Statistical analyses were performed using Student's t test: *p < 0.05 and ***p < 0.001. Scale bars: 5 µm (D and I) and 10 µm (G). See also Figure S2.

both genotypes (Figures S3C and S3D). This suggests that KIF21B, a potent microtubule growth-pausing factor (van Riel et al., 2017), constrains the dynamics of NBEA tubule motility.

Additional coIPs with either KIF21B or dynein intermediate chain (DIC)-specific antibodies identified triple association of NBEA, KIF21B, and DIC in brain lysates (Figure 3G). Immunodetection further revealed notable colocalization of both motors along neuronal dendrites (Pearson's correlation coefficient [PC] = 0.65 ± 0.03) (Figure S3E). In accordance with MS analysis (Table S1), endogenous NBEA and DIC were enriched at neuronal perinuclear compartments (Figure 3H) and frequently colocalized in dendritic processes (Figure 3I). We therefore examined NBEA motility following interference with dynein motor function by overexpressing dynamitin (Burkhardt et al., 1997). This led to a substantial reduction of mobile NBEA (Figures 3J and 3K), indicating that dynein motor function is requisite for NBEA motility. Thus, in contrast to KIF21B, dynein is involved in direct NBEA transport.

NBEA Is Located at Tubular Structures that Transiently Interact with Recycling Endosomes and Selectively Binds to Active Rab4

Because several Rab GTPases emerged in MS analysis (Table S1), we sought to determine the identity of the subcellular organelles that interact with NBEA. Among the Rab proteins assessed, GFP-NBEA displayed highest colocalization with tomato-Rab4-labeled recycling endosomes in COS-7 cells (Figures 4A and S4A), and 24.7% of endogenous NBEA colocalized with Rab4 in neurons (Figure 4B). GFP-NBEA and tomato-Rab4 signal peaks frequently overlapped at subcellular locations (Figure 4C; Video S4). Furthermore, IP with Rab4-specific antibodies co-precipitated endogenous NBEA from brain lysate (Figure 4H), indicating interaction of both factors. In neurons, time-lapse imaging revealed transient formation of NBEA tubule extensions at tomato-Rab4 vesicles (Figure 4D; Video S5). Interestingly, tubule extensions on individual endosomes grew out and fused

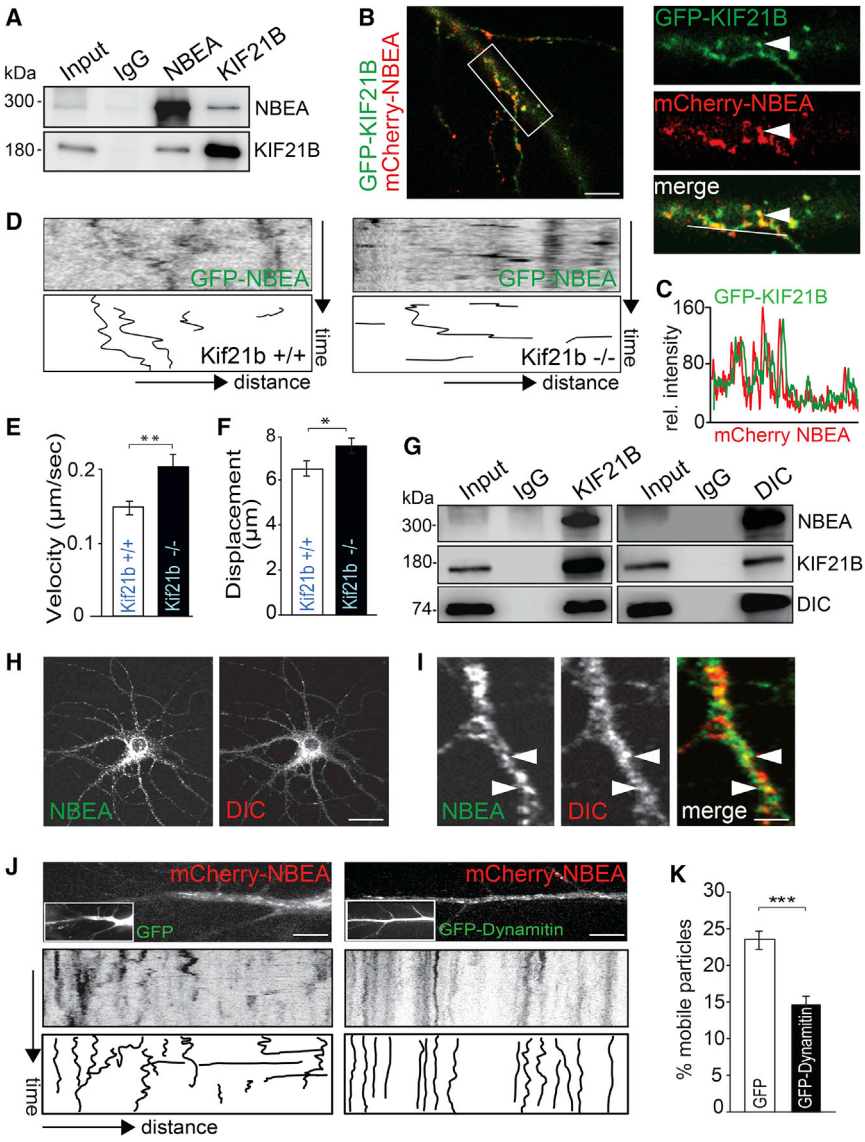

Figure 3. The Microtubule Motor Proteins KIF21B and Dynein Differentially Regulate Neurobeachin Motility

(A) CoIP of NBEA and KIF21B in vesicle-enriched (P3) brain lysate.

(B) Colocalization of GFP-KIF21B and mCherry-NBEA in neurons. Boxed region: dendritic segment shown to the right.

(C) Fluorescence intensity scan of white line in (B) depicting overlapping signal peaks.

(D) Kymographs of GFP-NBEA particle mobility in neurons derived from *Kif21b* wild-type (+/+) or knockout (−/−) mice.

(E) Quantification of GFP-NBEA velocity (n = 19 cells [+/+], n = 14 cells [−/−], n = 3 experiments; values represent mean ± SEM; **p < 0.01, Mann-Whitney U test).

(F) Quantification of GFP-NBEA displacement (n = 19 cells [+/+], n = 14 cells [−/−], n = 3 experiments; values represent mean ± SEM; *p < 0.05, Mann-Whitney U test).

(G) CoIP of NBEA, KIF21B, and DIC in vesicle-enriched (P3) brain lysate.

(H and I) Colocalization of endogenous NBEA (green) and endogenous DIC (red) in neurons (H) and dendrites (I). Arrowheads denote colocalized puncta.

(J) Still images and kymographs of neurons co-expressing mCherry-NBEA with either GFP (control, left) or the functional dynein inhibitor GFP-dynamitin (right). Small inset: green channel.

(K) Quantification of GFP-NBEA particle mobility (n = 47 cells [GFP], n = 45 cells [GFP-dynamitin], n = 3 experiments; values represent mean ± SEM; ***p < 0.001, Student's t test).

Scale bars: 2 µm (I), 5 µm (B and J), 20 µm (H). See also Figure S3.

back shortly after (Figure 4E), and a fraction of colocalized Rab4/NBEA puncta (24%) were cotransported over time (Figure 4F). To determine whether NBEA interacts with Rab4 in its active form, we performed coIPs following overexpression of either constitutively active Rab4 (mChRab4CA) or dominant-negative Rab4 (mChRab4DN). NBEA-specific antibodies precipitated NBEA (Figure 4G, top), whereas co-precipitation of mCherry-Rab4 was restricted to its constitutively active form (Figure 4G, bottom). To determine a role for NBEA at Rab4 recycling endosomes (Stenmark, 2009), we used short hairpin RNA (shRNA)-based NBEA knockdown in N2a cells (Figures S4B and S4C) and assessed the speed and displacement of Rab4-positive particles. Converse to the GFP-NBEA overexpression findings (Video S4), NBEA knockdown increased the speed and distance of Rab4 vesicles (Figures 4I–4L), indicating a role for NBEA in regulating Rab4 endosome dynamics.

NBEA Dynamically Interacts with Retromer and Golgi Proteins

Next, we assessed whether Rab4-specific antibodies might co-precipitate a larger endosomal complex consisting of Rab4, NBEA, and the motors identified (Figure 3). Indeed, Rab4 antibodies co-precipitated NBEA, KIF21B, and DIC from brain lysate (Figure 5A), indicating a link for kinesin KIF21B with recycling endosomes. In contrast, the kinesin KIF17 did not bind to Rab4 GTPases (Figure 5A).

In the Rab4-NBEA complex, we also detected the retromer marker VPS35 (Figure 5B), which is involved in endosome-to-Golgi and endosome-to-plasma membrane recycling (Choy et al., 2014). Endogenous VPS35 and Rab4 colocalized with NBEA in dendrites (PC = 0.5 ± 0.02; Figures 5C and 5D). Time-lapse imaging with the endosome-to-Golgi transport marker GFP-EHD3 (Naslavsky et al., 2009) and mCherry-NBEA revealed colocalization at tubular structures (Figure S5A) and cotransport over time (Figure S5B). We also examined NBEA relative to the GTPase and Golgi marker ARF1, which is also involved in retrograde transport from endosomes to the TGN or plasma membrane (Nakai et al., 2013). In neurons, GFP-ARF1 colocalized prominently with mCherry-NBEA (Figure S5C), suggesting related

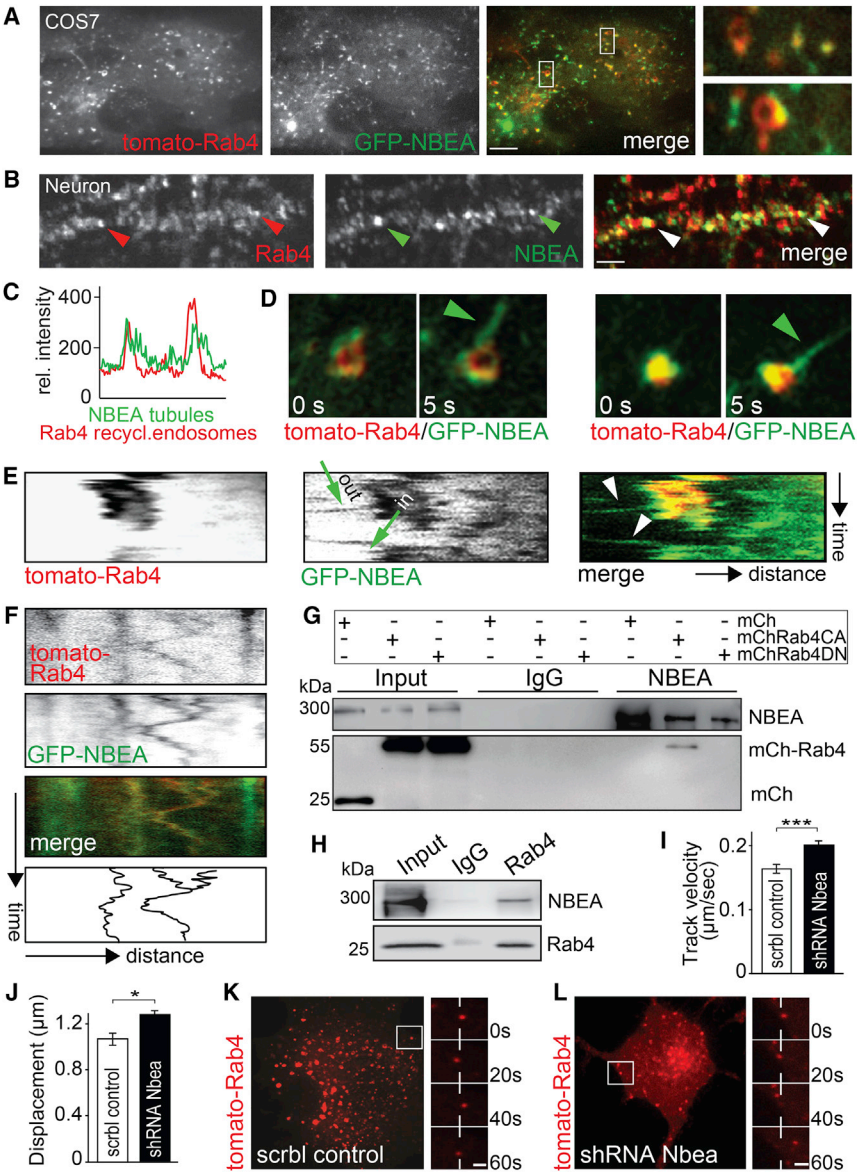

Figure 4. Neurobeachin Is Located to Tubular Structures Extending from Rab4-Positive Recycling Endosomes and Binds to Active Rab4

(A) Colocalization of tomato-Rab4 and GFP-NBEA in COS7 cells. Boxed regions are magnified (right).

(B) Colocalization of endogenous Rab4 (red) and endogenous NBEA (green) in DIV14 neurons (arrowheads) (n = 31 cells, n = 3 experiments).

(C) Fluorescence intensity scan depicting overlapping signal peaks from a representative region in (A).

(D) COS7 cells expressing tomato-Rab4 and GFP-NBEA. GFP-NBEA-positive tubules extend from tomato-Rab4 endosomes within 5 s (arrowhead).

(E) Kymograph from time-lapse recording of COS7 cells expressing GFP-NBEA and tomato-Rab4. GFP-NBEA-positive tubules extend and retract from tomato-Rab4 endosomes over time.

(F) Co-transport of GFP-NBEA and tomato-Rab4 in neurons (n = 39 cells, n = 3 experiments).

(G) CoIP experiments of GFP-NBEA with constitutively active (CA) or dominant-negative (DN) mCherry-Rab4 in HEK293 cells. Precipitation: anti-NBEA. GFP-NBEA exclusively binds to the active (CA) Rab4 variant.

(H) CoIP of endogenous Rab4 and endogenous NBEA from vesicle-enriched (P3) adult mouse brain lysate.

(I–L) Tomato-Rab4 mobility following shRNA-mediated NBEA knockdown in N2A cells. Quantification of velocity (I) and displacement (J) (n = 42 scrambled control cells, n = 40 shRNA cells, n = 4 experiments; values represent mean ± SEM; *p < 0.05 and ***p < 0.001, Mann-Whitney U test.) Boxed region in (K) and (L) enlarged to the right.

Scale bars: 2 µm (A, B, K, and L). See also Figure S4.

functions in trafficking regulation. Together, these findings suggest a role for NBEA at tubular and motor protein-regulated recycling organelles in the endosome-to-Golgi retrograde pathway.

NBEA Regulates Surface Membrane Recycling of GluN2B-Containing NMDARs

Because local dendritic Golgi satellite and retromer compartments recycle membrane proteins (Choy et al., 2014; Mikhaylova et al., 2016), we explored for candidate synaptic receptors that may undergo NBEA-dependent recycling. Based on NMDAR subunits identified in MS (Table S1), we used several NMDAR-specific antibodies to coIP NBEA from brain lysate (Figure S6). Also, reciprocal coIP identified GluN2B-containing NMDARs as NBEA interacting proteins (Figure 5E). The kinesin KIF17, which steers the synaptic delivery of newly synthesized GluN2B receptors (Yin et al., 2011), was not identified in this complex (Figure 5F). Endogenous colocalization analyses revealed that 24.4 ± 0.02% of NBEA signals overlapped with GluN2B. Also, 15.4 ± 1.7% of Rab4-positive recycling organelles were double-positive for NBEA and GluN2B (Figure 5G). In addition to GluN2B, endosomal NMDARs also contained GluN1 and GluN2A subunits (Figure 5H). Immunodetection revealed NBEA and GluN2B at spines opposed to synaptophysin-positive presynaptic terminals (Figure 5I), indicating colocalization at excitatory synapses. Finally, coIPs with GluN2B-specific antibodies precipitated the receptor, NBEA, VPS35, KIF21B, and DIC in brain lysate (Figures 6A and S6A), confirming that NMDARs are part of a motor-associated NBEA complex.

To assess whether NBEA regulates the recycling of GluN2B-containing NMDARs, we used a receptor-recycling assay based on cell surface biotinylation and co-streptavidin-precipitation in neurons derived from *Nbea* wild-type (+/+) and *Nbea*-knockout (−/−) mice (Figure 6G). Although the total receptor content was similar for both genotypes (Figure 6B), we detected more than 50% reduction of GluN2B-NMDAR cell surface levels in NBEA-knockout neurons (Figures 6C and S6E–S6G). This

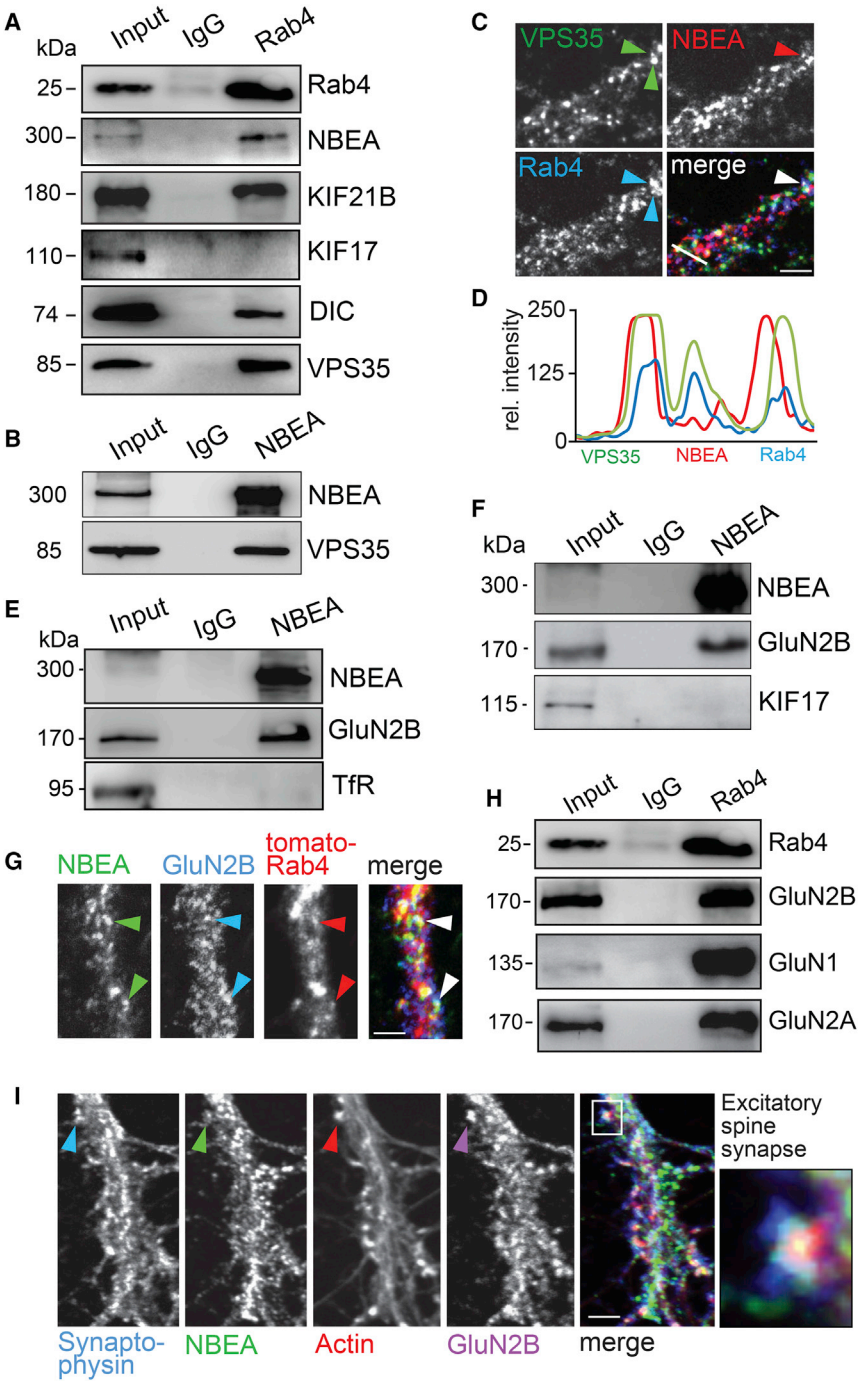

Figure 5. Neurobeachin Binds to and Colocalizes with a Retromer Component and NMDA Receptors

(A) CoIP of NBEA, KIF21B, DIC, and VPS35 with Rab4 in P3 vesicle-enriched fraction of adult mouse brain lysate. KIF17: negative control.

(B) CoIP of VPS35 with NBEA from P3 vesicle-enriched adult mouse brain lysate.

(C) Co-localization of endogenous VPS35, NBEA, and Rab4 in DIV14 neurons (arrowheads).

(D) Fluorescence intensity scan of white line in (C).

(E) CoIP of GluN2B, but not transferrin receptor (TfR) with NBEA from vesicle-enriched (P3) adult mouse brain extract.

(F) CoIP of GluN2B but not KIF17 with NBEA from vesicle-enriched (P3) adult mouse brain lysate.

(G) Co-localization of endogenous NBEA and GluN2B at tomato-Rab4-positive structures in DIV14 neurons (n = 14 cells).

(H) CoIP of GluN2B, GluN1, and GluN2A with Rab4 from vesicle-enriched (P3) adult mouse brain lysates.

(I) Co-localization of endogenous synaptophysin (blue), NBEA (green), actin (red), and GluN2B (purple) at excitatory synapses (n = 29 cells, n = 3 experiments).

Scale bars: 2 μm (C and G) and 5 μm (I). See also Figures S5 and S6.

corresponded with reduced NMDAR current amplitudes (Figures 6D–6F) and miniature excitatory postsynaptic current (mEPSC) frequencies (Figures S6B–S6D). Moreover, the ratio of internalized versus recycled GluN2B (internalized [block2]/not recycled [block3]) indicated significantly reduced recycling rates in NBEA-depleted neurons (Figures 6G–6I). This suggested that NBEA tubules participate in plasma membrane recycling of GluN2B-NMDARs. We also analyzed GluN2B-NMDAR cell surface levels following *Kif21b* knockout, because KIF21B regulates NBEA transport (Figure 3) and associates with NBEA and GluN2B (Figure 6A). Accordingly, GluN2B cell surface levels were significantly reduced in *Kif21b*-deficient slices (Figure 6J). NBEA knockdown compounded this effect in *Kif21b*-knockout neurons (Figures 6K, S4B, S4C, and S6J). In addition, *Kif21b* knockout increased coIP between NBEA and GluN2B in brain lysate (Figures S6H and S6I). Together, these findings indicate that NBEA and KIF21B cooperate to regulate NMDAR plasma membrane levels.

KIF21B Knockout Decreases Social Approach and Induces Social Cognitive Deficits

Qualitative impairment in social interest and interaction is a core symptom of ASDs (Poon and Sidhu, 2017). The *Nbea* and *Grin2b* genes are candidate ASD genes (Castermans et al., 2003; Nuytens et al., 2013; Pan et al., 2015) and are both relevant for cognitive function and social behavior in animal models (Nuytens et al., 2013; Wise et al., 2015; Wang et al., 2011). Our identification of a NBEA-KIF21B functional association in regulating GluN2B-NMDAR surface expression suggested that NBEA and KIF21B deficiency might induce similar phenotypes *in vivo*. Although *Kif21b*-knockout mice are impaired in learning and memory (Muhia et al., 2016), the role for KIF21B in social behavior is currently unknown.

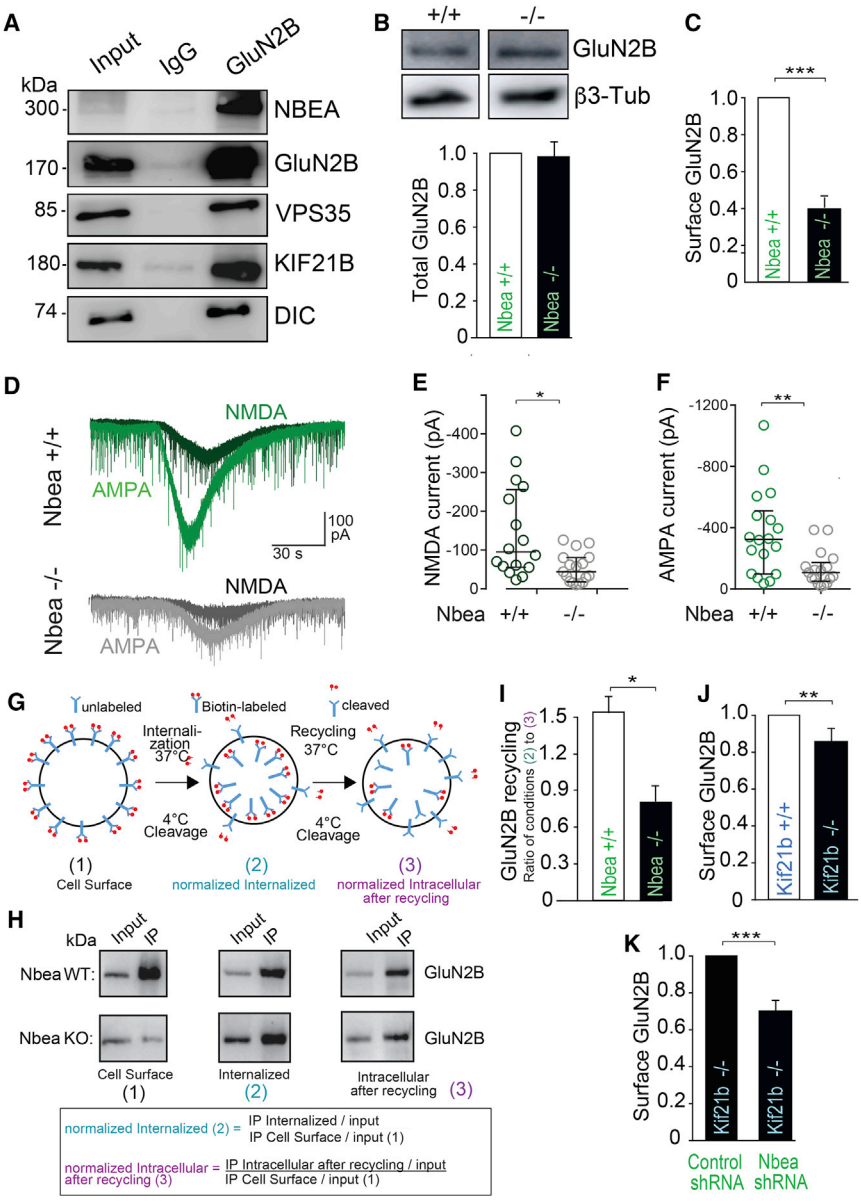

Figure 6. Neurobeachin Regulates Surface Membrane Recycling of GluN2B-Containing NMDA Receptors

(A) CoIP of NBEA, VPS35, KIF21B, and DIC with GluN2B in vesicle-enriched (P3) adult mouse brain extract.

(B) Quantification of total GluN2B protein content in *Nbea* wild-type (+/+) and knockout (−/−) neurons. β3-tubulin: loading control.

(C) Quantification of cell surface GluN2B levels in wild-type (+/+) and *Nbea*-knockout (−/−) neurons (values represent mean ± SEM; ***p < 0.001, Student's t test; n = 5 experiments).

(D) NBEA deficiency decreases NMDAR- and AMPAR-mediated currents in cultured hippocampal neurons.

(E and F) Quantification of representative responses to bath applied NMDA (E) and AMPA (F) in wild-type (+/+) neurons (green) and *Nbea*-knockout (−/−) neurons (gray). The median and interquartile range are indicated. *p ≤ 0.05 and **p ≤ 0.01, Mann-Whitney U test; n = 3 experiments.

(G–I) GluN2B recycling assay in wild-type (+/+) and *Nbea*-knockout (−/−) neurons.

(G) Schematic drawing: (1) Biotin-labeling prior to internalization. (2) Internalized receptors remain biotin-labeled. Biotin cleaved from non-internalized receptors. (3) Biotin cleavage at re-inserted receptors. Receptor recycling ratio expressed as internalized (block2) divided by non-recycled (block3).

(H) Western blot detection of GluN2B from steps 1–3 in (G) and formulas specifying how the measurements for GluN2B recycling ratio are achieved.

(I) Quantification of GluN2B recycled levels in wild-type (+/+) and NBEA-knockout (−/−) from (H) (values represent mean ± SEM; *p < 0.001, Student's t test; n = 5 experiments).

(J) Quantification of cell surface GluN2B levels in wild-type (+/+) and *Kif21b*-knockout (−/−) neurons (values represent mean ± SEM; **p < 0.01, Mann-Whitney U test; n = 4 experiments).

(K) Quantification of cell surface GluN2B levels in neurons transfected with NBEA shRNA (left) or scrambled control (right) constructs on the genetic background of *Kif21b*-knockout (−/−) mice (values represent mean ± SEM; ***p < 0.001, Mann-Whitney U test; n = 5 experiments).

See also Figure S6.

Therefore, we examined for the presence of ASD-related social phenotypes in *Kif21b*-knockout (−/−) mice by using the three-chamber social paradigm (Moy et al., 2004) (Figure 7A). Activity levels during initial acclimatization to the apparatus were comparable for both genotypes (Figure 7B). In the sociability phase, both genotypes showed overall biased preference for the novel conspecific over the inanimate object (Figures 7C and 7D). In accordance with the study in *Nbea*$^{+/-}$ mice (Nuytens et al., 2013), we examined interaction time during the initial phase of testing when novelty of the social stimulus is high. *Kif21b*$^{-/-}$ mice spent marginally significant less time actively exploring the cage containing the stranger mouse (Figure 7E), which suggested decreased tendency to approach the social target. In the subsequent social novelty phase, *Kif21b*$^{+/+}$ mice displayed a strong preference for the novel conspecific relative to the familiar mouse (Figures 7E and 7H, left). In contrast, *Kif21b*$^{-/-}$ mice showed diminished ability to differentiate between the familiar and novel mouse (Figures 7F–7I), indicating altered social recognition memory. Overall, *Kif21b*$^{-/-}$ mice displayed significantly decreased active exploration time with both social targets (Figures 7H and 7I), indicating that KIF21B knockout alters social behavior by interfering with social cognition as well as the initiation of social approach. The emergence of this phenotype is considered

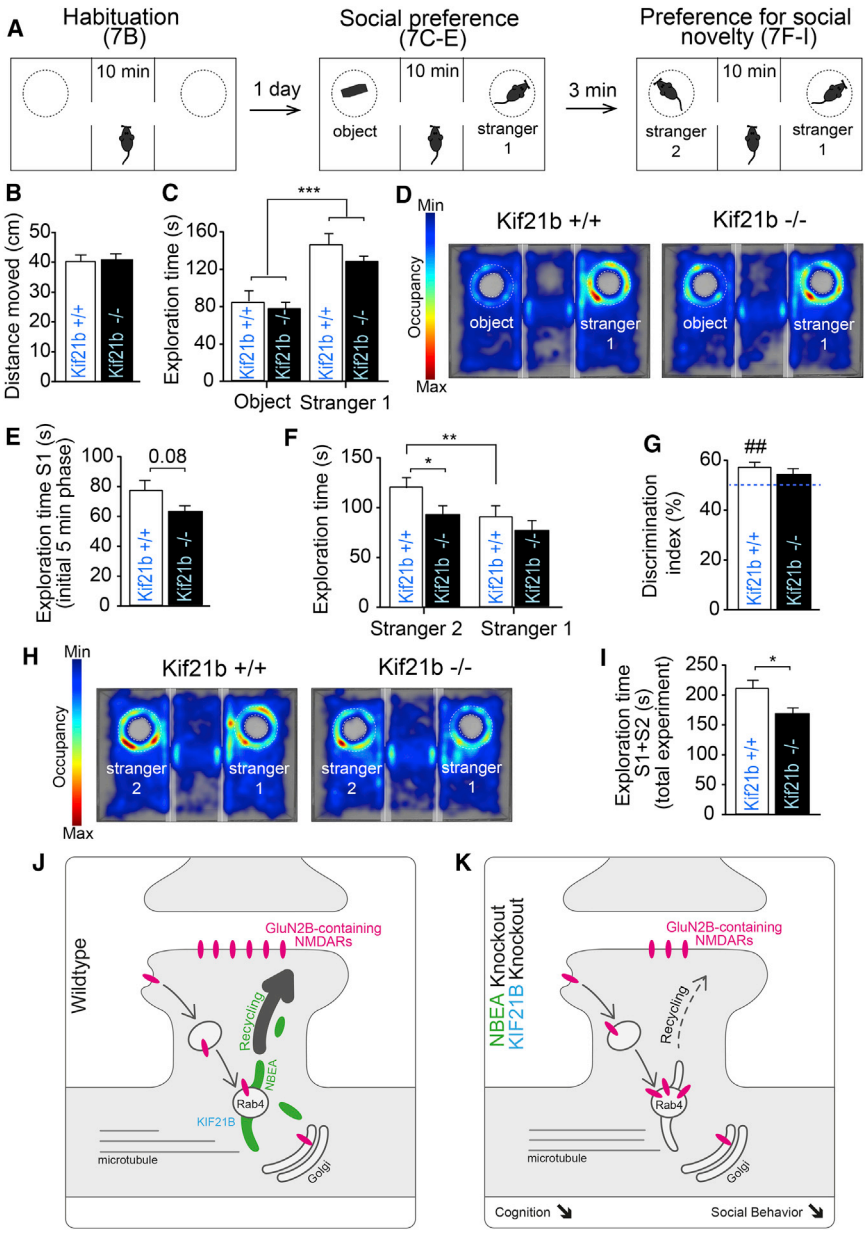

Figure 7. KIF21B Genetic Knockout in Mice Decreases Social Approach and Impairs Social Recognition

(A) Three-chambered mouse social paradigm to assess sociability and preference for social novelty (recognition memory).

(B) Activity levels during acclimatization to the apparatus are comparable (genotype: p = 0.86, univariate ANOVA).

(C–E) Social preference (sociability) test.

(C) Time spent in the vicinity of cage containing a novel conspecific (stranger 1) versus an inanimate object is significantly higher for both genotype groups (choice: ***p < 0.001, two-way repeated-measures [RM] ANOVA).

(D) *Kif21b*$^{-/-}$ mice showed marginally significant decreased exploration of the social target in the initial (5 min) phase of testing (genotype: p = 0.08, univariate ANOVA).

(E) Representative heatmaps illustrating mouse movement and exploration during the sociability phase. O, object; S1, stranger 1.

(F–I) Preference for social novelty as indexed by time spent in the vicinity of cage containing the familiar (stranger 1) versus the novel (stranger 2) mouse.

(F) *Kif21b*$^{-/-}$ mice failed to show preference for the novel over familiar mouse compared with controls (**p < 0.01, two-way ANOVA followed by restricted one-way ANOVA for each genotype group).

(G) *Kif21b*$^{+/+}$ mice demonstrated clear social recognition, as depicted by the discrimination index (time spent exploring stranger 2 [novel mouse] divided by total time spent exploring both mice × 100). This was at chance level in *Kif21b*$^{-/-}$ mice (##p < 0.01, one-sample t test against 50% chance level). Dotted line depicts chance level performance.

(H) Representative heatmaps illustrating mouse movement and exploration. S1, stranger 1; S2, stranger 2.

(I) Overall exploration time for both social targets were significantly lower for *Kif21b*$^{-/-}$ mice (genotype: *p < 0.05, univariate ANOVA). All data represent mean ± SEM.

(J and K) Hypothetical model: association of NBEA and KIF21B with components of the endosomal recycling machinery.

(J) NBEA (green) localizes to tubular structures, which transiently interact with Rab4-positive recycling endosomes (Figure 4) and enter synaptic spines in an activity-dependent manner (Figure 2). NBEA interacts with the microtubule motor protein KIF21B (blue) (Figure 3). NBEA functionally regulates plasma membrane recycling (bold arrow) of GluN2B-containing NMDA receptors (magenta) (Figure 6). Some NBEA particles undergo endosome-to-Golgi transport (Figure 5), indicating that NBEA participates in endosomal recycling.

(K) In the absence of NBEA, plasma membrane recycling (dashed arrow) and corresponding cell surface levels of GluN2B-containing NMDA receptors (magenta) are significantly reduced (Figure 6). Loss of the autism risk factor NBEA induces cognitive deficits and impaired social behavior in mice (Nuytens et al., 2013). Furthermore, genetic knockout of KIF21B, which acts as a microtubule pausing factor (Muhia et al., 2016; van Riel et al., 2017), leads to reduced NMDARs at the neuronal plasma membrane (Figure 6). Interestingly, *Kif21b*-knockout (−/−) mice also display deficits in cognitive function (Muhia et al., 2016), decreased social approach, and impaired social recognition (Figure 7). Our data suggest possible links between endocytic recycling and social behavior and highlight a molecular mechanism that may underlie ASD-related symptoms.

relevant to the ASD-like deficits in animal models (Silverman et al., 2010) and closely resembles the findings in *Nbea* (+/−) knockout mice (Nuytens et al., 2013). Thus, disruption of a common molecular NBEA-KIF21B mechanism may induce similar behavioral abnormalities in *Nbea* (+/−) and *Kif21b* (−/−) mice.

DISCUSSION

The present study demonstrates a role for NBEA in endosome dynamics and endocytic recycling of GluN2B-containing NMDARs. We show that NBEA associates with NMDAR subunits in a complex with endosomal recycling factors Rab4 GTPase

and VPS35 (Choy et al., 2014; Maxfield and McGraw, 2004; Stenmark, 2009). Importantly, NBEA is highly dynamic and located in mobile tubular vesicles that transiently fuse with and extend from Rab4 recycling endosomes. We show that NBEA regulates the recycling of internalized NMDARs and subsequent NMDAR synaptic targeting (Figure 6). Our study thus extends on the current role for NBEA in biosynthetic-to-plasma membrane trafficking (Wang et al., 2000), by yielding findings indicative of an additional role for NBEA in endocytic recycling of receptors. This is compatible with its detection at synaptic contacts (Figure 5) (Wang et al., 2000) and expression in the periphery of dendrites (Nair et al., 2013) suggesting local receptor targeting and/or re-insertion at the plasma membrane.

In light of the present findings, our emphasis is on the relevance for NBEA on NMDAR endocytic recycling, although the mechanism proposed here may be applicable to other receptor types (Figure 6) (Farzana et al., 2016; Nair et al., 2013). On the basis of previous suggestions for distinct NBEA-dependent roles in trafficking of different receptor types (Farzana et al., 2016; Nair et al., 2013), it is plausible that molecular interactions with discrete elements of the trafficking machinery (e.g., Table S1) may govern the specificity of NBEA-mediated trafficking of diverse membrane-bound cargo. In this regard, the NBEA-Rab4-VPS35 interaction identified here may be necessary for the specific recruitment of NBEA in regulating NMDAR endocytic recycling.

During synaptic activity, trafficking from recycling endosomes replenishes postsynaptic receptor content by shifting the steady-state equilibrium between intracellular compartments and the cell surface. For example, synaptic activity triggers Rab11 endosome delivery of AMPARs to synapses via myosin V and KIF1C motors (Correia et al., 2008; Esteves da Silva et al., 2015; Wang et al., 2008) and inhibition of endocytic recycling interferes with LTP (Park et al., 2004). Here, we identify NBEA as an additional factor in NMDAR endocytic recycling, thus extending on prior insight on NMDAR endocytic trafficking mechanisms (Cheng et al., 2013; Gu and Huganir, 2016; Piguel et al., 2014; Suh et al., 2010). The finding that NBEA entry into spines increases upon neuronal stimulation (Figure 2) is indicative of a role in the transport and re-insertion of receptors at synapses and concurs with its relevance to synaptic plasticity (Nuytens et al., 2013). This role may depend on transient and dynamic interactions between NBEA and Rab endosomes, consistent with the view that recycling endosomes act as a reserve pools in the rapid supply of receptors during synaptic plasticity (Kneussel and Hausrat, 2016).

While navigating along microtubules, motors can exert force on the membranes to which they are attached, leading to the formation of membrane tubules (Delevoye et al., 2014; Koster et al., 2003). Hence, different motors might associate with vesicular membranes to perform distinct functions (Hirokawa et al., 2010). Although dynein is implicated in endosomal transport, a role for kinesin KIF21B in endosomal trafficking is currently unclear. Here, we show that dynein motor function is requisite for direct NBEA transport. In contrast, KIF21B regulates the dynamics (velocity and displacement) of motile NBEA-containing tubules (Figure 3) as opposed to direct transport per se. This is consistent with its function on microtubule remodeling by enhancing microtubule catastrophes and pausing microtubule growth (Muhia et al., 2016; van Riel et al., 2017). KIF21B might therefore transiently constrain vesicles on the microtubule or may facilitate detachment of cargo from microtubule ends by initiating microtubule catastrophes in an activity-dependent manner (Ghiretti et al., 2016). Loss of detachment because of increased microtubule stability, for instance, may impair cargo unloading and contribute to the reduction of surface GluN2B and increased NBEA-GluN2B detection at vesicles in *Kif21b*-knockout brains (Figures S6H–S6J). Alternatively, lack of KIF21B might impair NBEA-dependent GluN2B-NMDAR surface delivery indirectly through its association with dynein (Figure 3G). Altogether, we propose a direct role for dynein in NBEA transport, whereas KIF21B plays a regulatory role on NBEA-containing vesicle dynamics through its selective influence on microtubule dynamics.

Because of the limited number of motors relative to intracellular cargo, motor proteins can transport multiple cargoes, which can in turn be transported by distinct motors (Hirokawa et al., 2010). In line with this, KIF21B is previously shown to affect the surface expression of different receptor types (Muhia et al., 2016) and may regulate $GABA_A$ receptor surface enrichment via E3 ubiquitin ligase TRIM3 (Labonté et al., 2013, 2014). Likewise, NBEA associates with several complexes (del Pino et al., 2011; Lauks et al., 2012) and regulates the trafficking and synaptic targeting of different receptor types (Farzana et al., 2016; Nair et al., 2013). Transport specificity critically depends on adaptor and effector proteins, which link motors to protein complexes to mediate cargo recognition and directionality of transport (Hirokawa et al., 2010; Kneussel et al., 2014). Dynein and kinesins are prominent Rab effectors and can associate directly or indirectly with Rab-GTPases (Horgan and McCaffrey, 2011). Here, we identify KIF21B as a component of the NBEA-Rab4-VPS35-GluN2B complex. The surface reduction of GluN2B in *Kif21b*-knockout neurons and mutual impact of KIF21B and NBEA deficiency on GluN2B-NMDAR surface expression (Figure 6) lends support for a NBEA-KIF21B functional interaction on NMDAR surface targeting. Thus, the NBEA-Rab4-KIF21B connection may mediate the specificity of KIF21B in regulating the dynamics of NMDAR recycling. Previous studies showed that kinesin KIF17 steers activity-dependent synaptic delivery of newly synthesized NMDARs (Yin et al., 2011, 2012). Contrary to KIF21B, KIF17 did not associate with Rab4 or NBEA (Figure 5), suggesting that the KIF17 and KIF21B may be distinctly recruited to regulate direct NMDAR transport and indirectly via influence on microtubule dynamics, respectively.

Studies have denoted the relevance for Rab-GTPase-mediated recycling to synaptic plasticity and cognitive function (Chiu et al., 2017; Hausser and Schlett, 2017). Besides their role in synaptic function and plasticity, GluN2B-NMDARs and NBEA are also essential for learning and memory (Nuytens et al., 2013; von Engelhardt et al., 2008; Yin et al., 2011). Endosomal systems are implicated in ASDs (Patak et al., 2016). Moreover, mutations in the *Nbea* and *Grin2b* genes are linked to ASDs in clinical studies (Castermans et al., 2003; Pan et al., 2015), including the relevance of both genes to ASD-like phenotypes in animal studies (Nuytens et al., 2013; Wang et al., 2011; Wise et al., 2015). Evidence indicates that GluN2B-NMDARs are

particularly essential to social memories (Jacobs et al., 2015). We have previously reported the relevance for KIF21B to synaptic function and learning and memory (Muhia et al., 2016). Our present findings at the cellular level suggests that NBEA and KIF21B might be elements of a common mechanism that underlies social behavior. In keeping with this, we show that *Kif21b* knockout decreases social approach and recognition (Figure 7). This deficit is relevant to the core social symptom in ASDs (Poon and Sidhu, 2017) and closely mimics the social deficits in *Nbea* mutants (Nuytens et al., 2013; Wise et al., 2015) and mice lacking GluN2B-NMDARs (Wang et al., 2011). Although we cannot rule out that alternative mechanisms might contribute to the overall phenotypes in the respective mutants, on the basis of the cellular findings reported here, it is reasonable to assume that the social deficits in *Kif21b*-knockout mice and elsewhere (Nuytens et al., 2013; Wang et al., 2011) might stem from interference of NBEA/KIF21B-mediated endocytic recycling of NMDARs.

Altogether, our study highlights an additional function for NBEA in the local delivery and re-insertion of synaptic proteins. We propose that KIF21B facilitates this process through its role on microtubule remodeling. NBEA-KIF21B functional interactions may therefore be relevant in efforts to understand the molecular mechanisms underlying ASD etiology.

EXPERIMENTAL PROCEDURES

Constructs and Antibodies

Constructs were verified by dideoxy sequencing. For details on plasmids and antibodies see Supplemental Experimental Procedures.

coIP and MS

Protein G-coupled Dynabeads were incubated with specific antibodies or control IgG. Antibody-coupled beads were incubated with brain lysates. After further processing, samples were analyzed by western blotting. For MS, proteins of a single experiment were digested with trypsin and analyzed using an UltiMate 3000 RSLCnano LC system connected to an LTQ Orbitrap Velos Pro mass spectrometer. Data were acquired using Xcalibur 2.2 software and processed with Proteome Discoverer. Raw MS/MS data were searched against the UniProtKB protein database. For details see Supplemental Experimental Procedures.

Primary Hippocampal Neuron Cultures, Transfection, and Immunohistochemistry

Hippocampal neuronal cultures were prepared from embryos (E16) and transfected using a calcium phosphate precipitation protocol. For immunostainings, neurons were fixed with 4% formaldehyde/4% sucrose in PBS. Confocal images were acquired using a confocal laser-scanning microscope with a 63× oil objective (Olympus, Hamburg, Germany). For details see Supplemental Experimental Procedures.

Live-Cell Imaging

Image acquisition was performed using a Nikon spinning disc confocal microscope equipped with 60× and 100× objectives, 488/561/614/405 nm lasers, and an incubation chamber (5% CO_2, 37°C). Images were captured every 1–3 s for 50–200 consecutive seconds. For details see Supplemental Experimental Procedures.

Mouse Behavioral Analysis

The generation of *Kif21b*-knockout (−/−) mice is described in detail elsewhere (Muhia et al., 2016). Experiments were carried out in accordance with German and European Union laws on the protection of experimental animals and following approval by the local authorities of the City of Hamburg (Committee for Lebensmittelsicherheit und Veterinärwesen, Authority of Soziales, Familie, Gesundheit und Verbraucherschutz Hamburg, Germany, No. 100/13). A cohort of 32 mice ($Kif21b^{+/+}$, n = 15 (8 females, 7 males]; $Kif21b^{-/-}$, n = 17 [9 males, 8 females]) was used to examine social behavior. For details see Supplemental Experimental Procedures.

Statistics

Statistical significance was assessed using Student's t test for parametric comparisons and the Mann-Whitney U test for non-parametric comparisons. Statistical analyses were performed using SigmaPlot 13.0 (Systat Software). Behavioral data were subjected to two-way or repeated-measures ANOVA whenever appropriate using SPSS version 21. Statistical significance was set at $p < 0.05$.

SUPPLEMENTAL INFORMATION

Supplemental Information includes Supplemental Experimental Procedures, six figures, one table, and five videos and can be found with this article online at https://doi.org/10.1016/j.celrep.2018.04.112.

ACKNOWLEDGMENTS

This work was supported by Deutsche Forschungsgemeinschaft (DFG) grants FOR 2419/P1 and KN556/11-1 and Landesforschungsförderung Hamburg (LFF) to M.K.; DFG grant FOR 2419/P4 and LFF to T.G.O.; and DFG grant FOR2410/P7 and LFF to C.E.G.

AUTHOR CONTRIBUTIONS

K.V.G. and M.K. designed the study. K.V.G., N.R., I.S., and C.E.G. performed experiments and analyzed the data with the help of E.T., T.G.O., and S.K. M.M. designed and performed behavioral experiments. O.S. performed MS and analyzed the data. M.W.K. contributed NBEA-knockout mice. K.V.G., M.M., and M.K. analyzed the data and wrote the manuscript with help of M.W.K. All authors read and commented on the manuscript.

DECLARATION OF INTERESTS

The authors declare no competing interests.

Received: May 30, 2017
Revised: February 20, 2018
Accepted: April 25, 2018
Published: May 29, 2018

REFERENCES

Burkhardt, J.K., Echeverri, C.J., Nilsson, T., and Vallee, R.B. (1997). Overexpression of the dynamitin (p50) subunit of the dynactin complex disrupts dynein-dependent maintenance of membrane organelle distribution. J. Cell Biol. *139*, 469–484.

Castermans, D., Wilquet, V., Parthoens, E., Huysmans, C., Steyaert, J., Swinnen, L., Fryns, J.P., Van de Ven, W., and Devriendt, K. (2003). The neurobeachin gene is disrupted by a translocation in a patient with idiopathic autism. J. Med. Genet. *40*, 352–356.

Cheng, J., Liu, W., Duffney, L.J., and Yan, Z. (2013). SNARE proteins are essential in the potentiation of NMDA receptors by group II metabotropic glutamate receptors. J. Physiol. *591*, 3935–3947.

Chiu, S.L., Diering, G.H., Ye, B., Takamiya, K., Chen, C.M., Jiang, Y., Niranjan, T., Schwartz, C.E., Wang, T., and Huganir, R.L. (2017). GRASP1 regulates synaptic plasticity and learning through endosomal recycling of AMPA receptors. Neuron *93*, 1405–1419.e8.

Choy, R.W., Park, M., Temkin, P., Herring, B.E., Marley, A., Nicoll, R.A., and von Zastrow, M. (2014). Retromer mediates a discrete route of local membrane delivery to dendrites. Neuron *82*, 55–62.

Collingridge, G.L., Isaac, J.T., and Wang, Y.T. (2004). Receptor trafficking and synaptic plasticity. Nat. Rev. Neurosci. *5*, 952–962.

Correia, S.S., Bassani, S., Brown, T.C., Lisé, M.F., Backos, D.S., El-Husseini, A., Passafaro, M., and Esteban, J.A. (2008). Motor protein-dependent transport of AMPA receptors into spines during long-term potentiation. Nat. Neurosci. *11*, 457–466.

de Souza, N., Vallier, L.G., Fares, H., and Greenwald, I. (2007). SEL-2, the C. elegans neurobeachin/LRBA homolog, is a negative regulator of lin-12/Notch activity and affects endosomal traffic in polarized epithelial cells. Development *134*, 691–702.

del Pino, I., Paarmann, I., Karas, M., Kilimann, M.W., and Betz, H. (2011). The trafficking proteins Vacuolar Protein Sorting 35 and Neurobeachin interact with the glycine receptor β-subunit. Biochem. Biophys. Res. Commun. *412*, 435–440.

Delevoye, C., Miserey-Lenkei, S., Montagnac, G., Gilles-Marsens, F., Paul-Gilloteaux, P., Giordano, F., Waharte, F., Marks, M.S., Goud, B., and Raposo, G. (2014). Recycling endosome tubule morphogenesis from sorting endosomes requires the kinesin motor KIF13A. Cell Rep. *6*, 445–454.

Esteves da Silva, M., Adrian, M., Schätzle, P., Lipka, J., Watanabe, T., Cho, S., Futai, K., Wierenga, C.J., Kapitein, L.C., and Hoogenraad, C.C. (2015). Positioning of AMPA receptor-containing endosomes regulates synapse architecture. Cell Rep. *13*, 933–943.

Farzana, F., Zalm, R., Chen, N., Li, K.W., Grant, S.G., Smit, A.B., Toonen, R.F., and Verhage, M. (2016). Neurobeachin regulates glutamate- and GABA-receptor targeting to synapses via distinct pathways. Mol. Neurobiol. *53*, 2112–2123.

Ghiretti, A.E., Thies, E., Tokito, M.K., Lin, T., Ostap, E.M., Kneussel, M., and Holzbaur, E.L.F. (2016). Activity-dependent regulation of distinct transport and cytoskeletal remodeling functions of the dendritic kinesin KIF21B. Neuron *92*, 857–872.

Granger, A.J., Shi, Y., Lu, W., Cerpas, M., and Nicoll, R.A. (2013). LTP requires a reserve pool of glutamate receptors independent of subunit type. Nature *493*, 495–500.

Gu, Y., and Huganir, R.L. (2016). Identification of the SNARE complex mediating the exocytosis of NMDA receptors. Proc. Natl. Acad. Sci. U S A *113*, 12280–12285.

Guillaud, L., Wong, R., and Hirokawa, N. (2008). Disruption of KIF17-Mint1 interaction by CaMKII-dependent phosphorylation: a molecular model of kinesin-cargo release. Nat. Cell Biol. *10*, 19–29.

Hausser, A., and Schlett, K. (2017). Coordination of AMPA receptor trafficking by Rab GTPases. Small GTPases, Published online June 19, 2017. https://doi.org/10.1080/21541248.2017.1337546.

Hirokawa, N., Niwa, S., and Tanaka, Y. (2010). Molecular motors in neurons: transport mechanisms and roles in brain function, development, and disease. Neuron *68*, 610–638.

Horgan, C.P., and McCaffrey, M.W. (2011). Rab GTPases and microtubule motors. Biochem. Soc. Trans. *39*, 1202–1206.

Hu, X., Viesselmann, C., Nam, S., Merriam, E., and Dent, E.W. (2008). Activity-dependent dynamic microtubule invasion of dendritic spines. J. Neurosci. *28*, 13094–13105.

Huganir, R.L., and Nicoll, R.A. (2013). AMPARs and synaptic plasticity: the last 25 years. Neuron *80*, 704–717.

Jacobs, S., Wei, W., Wang, D., and Tsien, J.Z. (2015). Importance of the GluN2B carboxy-terminal domain for enhancement of social memories. Learn. Mem. *22*, 401–410.

Kneussel, M., and Hausrat, T.J. (2016). Postsynaptic neurotransmitter receptor reserve pools for synaptic potentiation. Trends Neurosci. *39*, 170–182.

Kneussel, M., Triller, A., and Choquet, D. (2014). SnapShot: receptor dynamics at plastic synapses. Cell *157*, 1738–1738.e1.

Koster, G., VanDuijn, M., Hofs, B., and Dogterom, M. (2003). Membrane tube formation from giant vesicles by dynamic association of motor proteins. Proc. Natl. Acad. Sci. U S A *100*, 15583–15588.

Labonté, D., Thies, E., Pechmann, Y., Groffen, A.J., Verhage, M., Smit, A.B., van Kesteren, R.E., and Kneussel, M. (2013). TRIM3 regulates the motility of the kinesin motor protein KIF21B. PLoS ONE *8*, e75603.

Labonté, D., Thies, E., and Kneussel, M. (2014). The kinesin KIF21B participates in the cell surface delivery of γ2 subunit-containing GABAA receptors. Eur. J. Cell Biol. *93*, 338–346.

Lauks, J., Klemmer, P., Farzana, F., Karupothula, R., Zalm, R., Cooke, N.E., Li, K.W., Smit, A.B., Toonen, R., and Verhage, M. (2012). Synapse associated protein 102 (SAP102) binds the C-terminal part of the scaffolding protein neurobeachin. PLoS ONE *7*, e39420.

Maxfield, F.R., and McGraw, T.E. (2004). Endocytic recycling. Nat. Rev. Mol. Cell Biol. *5*, 121–132.

Medrihan, L., Rohlmann, A., Fairless, R., Andrae, J., Döring, M., Missler, M., Zhang, W., and Kilimann, M.W. (2009). Neurobeachin, a protein implicated in membrane protein traffic and autism, is required for the formation and functioning of central synapses. J. Physiol. *587*, 5095–5106.

Mikhaylova, M., Bera, S., Kobler, O., Frischknecht, R., and Kreutz, M.R. (2016). A dendritic Golgi satellite between ERGIC and retromer. Cell Rep. *14*, 189–199.

Moy, S.S., Nadler, J.J., Perez, A., Barbaro, R.P., Johns, J.M., Magnuson, T.R., Piven, J., and Crawley, J.N. (2004). Sociability and preference for social novelty in five inbred strains: an approach to assess autistic-like behavior in mice. Genes Brain Behav. *3*, 287–302.

Muhia, M., Thies, E., Labonté, D., Ghiretti, A.E., Gromova, K.V., Xompero, F., Lappe-Siefke, C., Hermans-Borgmeyer, I., Kuhl, D., Schweizer, M., et al. (2016). The kinesin KIF21B regulates microtubule dynamics and is essential for neuronal morphology, synapse function, and learning and memory. Cell Rep. *15*, 968–977.

Nair, R., Lauks, J., Jung, S., Cooke, N.E., de Wit, H., Brose, N., Kilimann, M.W., Verhage, M., and Rhee, J. (2013). Neurobeachin regulates neurotransmitter receptor trafficking to synapses. J. Cell Biol. *200*, 61–80.

Nakai, W., Kondo, Y., Saitoh, A., Naito, T., Nakayama, K., and Shin, H.W. (2013). ARF1 and ARF4 regulate recycling endosomal morphology and retrograde transport from endosomes to the Golgi apparatus. Mol. Biol. Cell *24*, 2570–2581.

Naslavsky, N., McKenzie, J., Altan-Bonnet, N., Sheff, D., and Caplan, S. (2009). EHD3 regulates early-endosome-to-Golgi transport and preserves Golgi morphology. J. Cell Sci. *122*, 389–400.

Niesmann, K., Breuer, D., Brockhaus, J., Born, G., Wolff, I., Reissner, C., Kilimann, M.W., Rohlmann, A., and Missler, M. (2011). Dendritic spine formation and synaptic function require neurobeachin. Nat. Commun. *2*, 557.

Nuytens, K., Gantois, I., Stijnen, P., Iscru, E., Laeremans, A., Serneels, L., Van Eylen, L., Liebhaber, S.A., Devriendt, K., Balschun, D., et al. (2013). Haploinsufficiency of the autism candidate gene Neurobeachin induces autism-like behaviors and affects cellular and molecular processes of synaptic plasticity in mice. Neurobiol. Dis. *51*, 144–151.

Pan, Y., Chen, J., Guo, H., Ou, J., Peng, Y., Liu, Q., Shen, Y., Shi, L., Liu, Y., Xiong, Z., et al. (2015). Association of genetic variants of GRIN2B with autism. Sci. Rep. *5*, 8296.

Park, M., Penick, E.C., Edwards, J.G., Kauer, J.A., and Ehlers, M.D. (2004). Recycling endosomes supply AMPA receptors for LTP. Science *305*, 1972–1975.

Patak, J., Zhang-James, Y., and Faraone, S.V. (2016). Endosomal system genetics and autism spectrum disorders: A literature review. Neurosci. Biobehav. Rev. *65*, 95–112.

Petrini, E.M., Lu, J., Cognet, L., Lounis, B., Ehlers, M.D., and Choquet, D. (2009). Endocytic trafficking and recycling maintain a pool of mobile surface AMPA receptors required for synaptic potentiation. Neuron *63*, 92–105.

Piguel, N.H., Fievre, S., Blanc, J.M., Carta, M., Moreau, M.M., Moutin, E., Pinheiro, V.L., Medina, C., Ezan, J., Lasvaux, L., et al. (2014). Scribble1/AP2 complex coordinates NMDA receptor endocytic recycling. Cell Rep. *9*, 712–727.

Poon, K.K., and Sidhu, D.J. (2017). Adults with autism spectrum disorders: a review of outcomes, social attainment, and interventions. Curr. Opin. Psychiatry *30*, 77–84.

Sheff, D.R., Daro, E.A., Hull, M., and Mellman, I. (1999). The receptor recycling pathway contains two distinct populations of early endosomes with different sorting functions. J. Cell Biol. *145*, 123–139.

Silverman, J.L., Yang, M., Lord, C., and Crawley, J.N. (2010). Behavioural phenotyping assays for mouse models of autism. Nat. Rev. Neurosci. *11*, 490–502.

Stenmark, H. (2009). Rab GTPases as coordinators of vesicle traffic. Nat. Rev. Mol. Cell Biol. *10*, 513–525.

Suh, Y.H., Terashima, A., Petralia, R.S., Wenthold, R.J., Isaac, J.T., Roche, K.W., and Roche, P.A. (2010). A neuronal role for SNAP-23 in postsynaptic glutamate receptor trafficking. Nat. Neurosci. *13*, 338–343.

van der Sluijs, P., and Hoogenraad, C.C. (2011). New insights in endosomal dynamics and AMPA receptor trafficking. Semin. Cell Dev. Biol. *22*, 499–505.

van Riel, W.E., Rai, A., Bianchi, S., Katrukha, E.A., Liu, Q., Heck, A.J., Hoogenraad, C.C., Steinmetz, M.O., Kapitein, L.C., and Akhmanova, A. (2017). Kinesin-4 KIF21B is a potent microtubule pausing factor. eLife *6*, 6.

von Engelhardt, J., Doganci, B., Jensen, V., Hvalby, Ø., Göngrich, C., Taylor, A., Barkus, C., Sanderson, D.J., Rawlins, J.N., Seeburg, P.H., et al. (2008). Contribution of hippocampal and extra-hippocampal NR2B-containing NMDA receptors to performance on spatial learning tasks. Neuron *60*, 846–860.

Wang, X., Herberg, F.W., Laue, M.M., Wullner, C., Hu, B., Petrasch-Parwez, E., and Kilimann, M.W. (2000). Neurobeachin: a protein kinase A-anchoring, beige/Chediak-higashi protein homolog implicated in neuronal membrane traffic. J. Neurosci. *20*, 8551–8565.

Wang, Z., Edwards, J.G., Riley, N., Provance, D.W., Jr., Karcher, R., Li, X.D., Davison, I.G., Ikebe, M., Mercer, J.A., Kauer, J.A., and Ehlers, M.D. (2008). Myosin Vb mobilizes recycling endosomes and AMPA receptors for postsynaptic plasticity. Cell *135*, 535–548.

Wang, C.C., Held, R.G., Chang, S.C., Yang, L., Delpire, E., Ghosh, A., and Hall, B.J. (2011). A critical role for GluN2B-containing NMDA receptors in cortical development and function. Neuron *72*, 789–805.

Wise, A., Tenezaca, L., Fernandez, R.W., Schatoff, E., Flores, J., Ueda, A., Zhong, X., Wu, C.F., Simon, A.F., and Venkatesh, T. (2015). Drosophila mutants of the autism candidate gene neurobeachin (rugose) exhibit neuro-developmental disorders, aberrant synaptic properties, altered locomotion, and impaired adult social behavior and activity patterns. J. Neurogenet. *29*, 135–143.

Yin, X., Takei, Y., Kido, M.A., and Hirokawa, N. (2011). Molecular motor KIF17 is fundamental for memory and learning via differential support of synaptic NR2A/2B levels. Neuron *70*, 310–325.

Yin, X., Feng, X., Takei, Y., and Hirokawa, N. (2012). Regulation of NMDA receptor transport: a KIF17-cargo binding/releasing underlies synaptic plasticity and memory in vivo. J. Neurosci. *32*, 5486–5499.